Earth Syst. Dynam., 7, 167–181, 2016
www.earth-syst-dynam.net/7/167/2016/
doi:10.5194/esd-7-167-2016

Earth System Dynamics
Open Access
EGU

The role of spatial scale and background climate in the latitudinal temperature response to deforestation

Yan Li[1,2,3,4], Nathalie De Noblet-Ducoudré[5], Edouard L. Davin[6], Safa Motesharrei[4,7,8], Ning Zeng[2], Shuangcheng Li[1,3], and Eugenia Kalnay[2,4]

[1]College of Urban and Environmental Sciences, Peking University, 100871 Beijing, China
[2]Department of Atmospheric and Oceanic Science, University of Maryland, College Park, Maryland 20742, USA
[3]Key Laboratory for Earth Surface Processes of The Ministry of Education, Peking University, 100871 Beijing, China
[4]The Institute for Physical Science and Technology, University of Maryland, College Park, Maryland 20742, USA
[5]Laboratoire des Sciences du Climat et de l'Environnement, Institut Unité Mixte CEA-CNRS-UVSQ, Université Paris-Saclay, Orme des Merisiers, Bât. 712, 91191 Gif-sur-Yvette, France
[6]Institute for Atmospheric and Climate Science, Eidgenössiche Technische Hochschule (ETH) Zurich, 8092 Zurich, Switzerland
[7]Department of Physics, University of Maryland, College Park, Maryland 20742, USA
[8]National Socio-Environmental Synthesis Center (SESYNC), Annapolis, Maryland 21401, USA

Correspondence to: Yan Li (yanli.geo@gmail.com)

Received: 5 September 2015 – Published in Earth Syst. Dynam. Discuss.: 9 October 2015
Revised: 29 January 2016 – Accepted: 18 February 2016 – Published: 7 March 2016

Abstract. Previous modeling and empirical studies have shown that the biophysical impact of deforestation is to warm the tropics and cool the extratropics. In this study, we use an earth system model of intermediate complexity to investigate how deforestation on various spatial scales affects ground temperature, with an emphasis on the latitudinal temperature response and its underlying mechanisms. Results show that the latitudinal pattern of temperature response depends nonlinearly on the spatial extent of deforestation and the fraction of vegetation change. Compared with regional deforestation, temperature change in global deforestation is greatly amplified in temperate and boreal regions but is dampened in tropical regions. Incremental forest removal leads to increasingly larger cooling in temperate and boreal regions, while the temperature increase saturates in tropical regions. The latitudinal and spatial patterns of the temperature response are driven by two processes with competing temperature effects: decrease in absorbed shortwave radiation due to increased albedo and decrease in evapotranspiration. These changes in the surface energy balance reflect the importance of the background climate in modifying the deforestation impact. Shortwave radiation and precipitation have an intrinsic geographical distribution that constrains the effects of biophysical changes and therefore leads to temperature changes that are spatially varying. For example, wet (dry) climate favors larger (smaller) evapotranspiration change; thus, warming (cooling) is more likely to occur. Our analysis reveals that the latitudinal temperature change largely results from the climate conditions in which deforestation occurs and is less influenced by the magnitude of individual biophysical changes such as albedo, roughness, and evapotranspiration efficiency.

1 Introduction

Forests play a critical role in regulating climate through both biogeochemical and biophysical processes. Deforestation – driven by anthropogenic activities either directly, e.g., by agriculture expansion, or indirectly, e.g., by climate-change-induced disturbance (Allen et al., 2010) – can result in changes in earth's radiation balance, hydrological cycle, and atmospheric composition (Bonan, 2008). Deforestation is a major land conversion that has taken place historically over large scales and continues to be prevalent in the 21st century (Hansen et al., 2013).

Previous climate model studies highlight the interesting observation that temperature response to deforestation appears to depend on latitude (Davin and de Noblet-Ducoudré, 2010). For example, large-scale deforestation in the tropics leads to temperature increase (Nobre et al., 1991; Snyder et al., 2004; Davin and de Noblet-Ducoudré, 2010) mostly due to the strong warming effect associated with reduced evapotranspiration. However, forest removal in the temperate and high-latitude regions results in surface temperature decrease. This decrease is explained by the dominant mechanism, albedo, which increases in the cleared land and leads to lower shortwave radiation absorption (Bounoua et al., 2002; Snyder et al., 2004). This albedo-induced cooling effect is particularly strong in the boreal regions where the snow mask effect is involved (Bonan et al., 1992, 1995). In agreement with the climate model experiments, empirical studies using in situ air temperature (Lee et al., 2011; Zhang et al., 2014) and satellite-derived land surface temperature (Li et al., 2015) also show that the temperature effects of forests have a clear latitudinal pattern.

Compared with biogeochemical effects, i.e., release of CO_2 to the atmosphere that warms the global climate, biophysical effects are more heterogeneous, are most strongly felt at regional and local levels (Bala et al., 2007; Pitman et al., 2012), and vary with season and location (Snyder et al., 2004; Betts et al., 2007; Li et al., 2015). It is thought that biophysical effects, especially albedo and evapotranspiration, are major biophysical mechanisms through which deforestation affects temperature in latitudinal patterns (Gibbard et al., 2005). However, due to the high spatial variability of biophysical properties, the dominant mechanism and the net effect of deforestation could vary by particular location. This is further complicated by the influence of specific location's background climate on the altered water and energy balance. For example, previous studies show that climate conditions, such as snow and rainfall, can enhance or dampen biophysical effects (Pitman et al., 2011; Li et al., 2015). Such complexity is reflected in temperate forests, where the two biophysical mechanisms with opposite effects cancel each other, making their net effect much more uncertain compared to other forests. This incomplete understanding of temperate forests was confirmed by the mixed results obtained from modeling and observational studies (Bonan, 2008; Wickham et al., 2013; Li et al., 2015). Further complication comes from deforestation-triggered changes in other energy components (such as sensible heat) and multiple atmospheric feedbacks that can modify the albedo and evapotranspiration impact. Therefore, it is important to further investigate the relative strength of albedo and evapotranspiration impact on temperature change and how much those factors are influenced by the interaction with the local climate and other factors.

In addition to these biophysical effects, the spatial scale of deforestation is also an important factor in climatic impact. It has been shown that both spatial extent (global–regional–local) and degree of vegetation change (partial disturbance to complete removal) can alter the impact of deforestation (Sampaio et al., 2007; Longobardi et al., 2012). Evidence for this behavior is seen in the Amazon area, where depending on the spatial scale of deforestation, precipitation change can either exhibit a linear or nonlinear relationship with vegetation change (Avissar et al., 2002; Baidya Roy and Avissar, 2002; Souza and Oyama, 2010). And this relationship could even become opposite in sign (Runyan, 2012). The effect of vegetation change on various scales is still not clear on either the scale dependency or latitudinal pattern of temperature response.

As described, the impact on temperature as a result of deforestation originates from the altered biophysical properties such as albedo, roughness, canopy conductance, and surface emissivity. The magnitude of some of these alterations, as well as their impact on temperature, may have inherent latitudinal patterns. For instance, the difference in albedo between forest and open land increases with latitude (Li et al., 2015). By investigating how changes to several biophysical properties contribute to temperature change, we can better understand whether the latitudinal temperature response to deforestation is either directly due to these changes or to the processes that translate these changes in the surface climate response. Efforts have been made to quantify the contribution of each biophysical factor, including both empirical (Juang et al., 2007) and modeling studies (Lean and Rowntree, 1997; Maynard and Royer, 2004; Davin and de Noblet-Ducoudré, 2010) that enable us to decompose the temperature change into components. Such studies can improve our knowledge on the mechanisms of the climate impact induced by vegetation change.

In this study, we use an earth system model of intermediate complexity (EMIC) to investigate how deforestation affects temperature through biophysical changes and also examine which physical mechanisms are responsible for the latitude-dependent temperature response (Sect. 2). To this aim, we first analyze latitudinal temperature changes in response to multiple deforestation scenarios by varying both spatial extent and deforestation fraction (Sects. 3.1 and 3.2). Next, we explore the possible causes for the latitudinal and spatial pattern of temperature change from both the surface energy balance (Sect. 3.3), as well as the background climate

(Sect. 3.4). Finally, we show how different biophysical mechanisms affect temperature change and discuss their contributions to the latitudinal pattern (Sect. 3.5). A brief discussion and summary are provided in Sect. 4.

2 Method

2.1 Model description

The UMD (University of Maryland) EMIC (Zeng, 2004) is used to perform the experiments. It consists of the global version of the atmosphere QTCM (Quasi-Equilibrium Tropical Circulation Model) (Neelin and Zeng, 2000), the physical land surface model Sland (Simple land) (Zeng et al., 2000), the dynamic vegetation and carbon model VEGAS (VEgetation–Global–Atmosphere–Soil) (Zeng, 2003; Zeng et al., 2005), and a slab ocean model in which we use prescribed sea surface temperatures (SSTs) in our experiments.

Sland is a land surface model of intermediate complexity that is more complicated than the bucket model in its parameterization of evapotranspiration processes, aiming to model the first-order effects relevant to climate simulation. In this model, vegetation parameters such as leaf area index, roughness, stomatal conductance, and vegetation fraction depend on climate and are calculated by VEGAS. For surface albedo, seasonal climatology obtained from satellite is used as inputs (Darnell et al., 1992). Vegetation-albedo feedback is treated in the model by introducing albedo anomalies. This procedure sums the albedo change due to vegetation change (calculated by VEGAS using an empirical formula as a function of leaf area index, LAI) and the observed albedo climatology used by the atmospheric radiation module (Zeng and Yoon, 2009). This albedo anomalies treatment prioritizes the capture of the first-order effects of albedo change due to vegetation change, since many of the possible processes that are responsible for the observed albedo are difficult to model mechanistically.

It should be mentioned that Sland in its current setup does not explicitly account for surface snow; thus, no snow-albedo feedback is included. This potentially leads to an underestimation of albedo change in regions with frequent snow. However, it also offers a unique opportunity to examine mechanisms other than snow in the temperature response to deforestation at high latitudes.

The VEGAS model simulates the dynamics of vegetation growth and competition among four plant functional types (PFTs): broadleaf tree, needleleaf tree, cold grass, and warm grass. The phenology of these plants is simulated dynamically as the balance between growth and respiration or turnover. The vegetation component is coupled to land and atmosphere through soil moisture dependence of photosynthesis and evapotranspiration, as well as dependence on temperature, radiation, and atmospheric CO_2. The UMD EMIC has been used to study the climate and vegetation feedbacks (e.g., Zeng et al., 1999; Zeng and Neelin, 2000; Hales et al., 2004; Zeng and Yoon, 2009) and contributed to C^4MIP, the Coupled Climate–Carbon Cycle Model Intercomparison Project (Friedlingstein et al., 2006).

2.2 Experiment design

UMD earth system model is a fully coupled model, but the setup for this study is an atmosphere–land–vegetation coupled version with prescribed ocean SST and CO_2 concentration at the preindustrial level of 280 ppm, run at a resolution of $5.625° \times 3.75°$. The model is driven by a climatological seasonal cycle of SST derived from HadSST (Rayner et al., 2006), averaged over 1960–1990 to smooth the influence of interannual climate variability. The model is first run for 500 years to allow for spin-up time, during which vegetation is dynamically computed and reaches an equilibrium state with climate. Figure S1 in the Supplement shows the potential vegetation map obtained by the end of model spin-up. The vegetation map generally has a reasonable geographical distribution but does not perfectly match the modern vegetation of the real world. This is expected because the potential vegetation is derived from an equilibrium state with climate. Therefore, any differences in the simulated climate compared to modern climate or any simulation bias, for example, in precipitation (Fig. S2 in the Supplement), could influence the vegetation distribution. In addition, some bias in simulated climate is expected for a model with intermediate complexity. Such bias is tolerable in our experiments due to the focus on the climate response to vegetation change and its mechanisms as opposed to an accurate reproduction of historical climate change. For our analysis, the climatology over the last 10 years of spin-up is used as the control experiment (CTL). This is adequate for our simulation because of the small interannual variability in the model.

Deforestation is imposed by setting the forest fraction in a given grid cell to the experimental value of either zero or a percentage of its original vegetation. This replaces the forest with bare soil, as is seen in several previous studies (Bonan et al., 1992; Gibbard et al., 2005; Snyder, 2010). An alternative strategy of implementing the deforestation experiment is to replace trees with grass (crop). This is considered to be more "realistic" than replacing trees with bare ground (Davin and de Noblet-Ducoudré, 2010). The conversion of trees to grass is expected to induce a similar but less pronounced impact on climate (Gibbard et al., 2005), compared to the conversion of trees to bare ground which would represent the maximum impact of deforestation. Despite this difference, both strategies are frequently used in existing literature to represent deforestation, and they yield consistent findings as the operating mechanisms and feedbacks are the same. In the simulation for the deforestation experiment, modified vegetation fractions are fixed so that the vegetation model becomes "static" rather than "dynamic".

Three groups of experiments are designed to study different aspects of the deforestation impact (Table 1): (I) de-

Table 1. Deforestation experiment design.

Group	I. Spatial extent	II. Deforestation fractions	III. Biophysical factors
Experiment	Tropical	25 % global forest removal	Albedo
	Temperate	50 % global forest removal	Roughness
	Boreal	75 % global forest removal	Evapotranspiration efficiency
	Global	100 % global forest removal	

forestation with different spatial extents; (II) with different deforestation fractions; (III) with individual biophysical factors changed separately. The first two groups address the spatial-scale problem for the climatic response to deforestation. Group (I) consists of three regional deforestation scenarios that take place in the tropical (20° S–20° N), northern temperate (20–50° N), and boreal (50–90° N) regions and one global deforestation scenario, in which all forests are cleared. Group (II) consists of four global deforestation experiments in which forest fractions are reduced as a percent (25 to 100 %) of the original forest coverage. The 100 % clearing creates the same experiment as the global deforestation in group I, labeled ALL.

Group (III) is designed to separate the effect of individual biophysical factors by which deforestation affects climate. Inspired by Davin and de Noblet-Ducoudré (2010), three experiments are devised to quantify the impact from changes in albedo, roughness, and evapotranspiration efficiency. Our experiment for albedo and roughness differs from Davin and de Noblet-Ducoudré (2010), who compared the case with only "one factor changed" with the case of "everything unchanged". In contrast, we ultimately compare the case of "everything changed with one factor unchanged" with the case of "everything changed". Our experiments include global deforestation with albedo unchanged in "noALB", roughness unchanged in "noRGH", and evapotranspiration efficiency effect isolated in "EVA". In the noALB experiment, albedo change induced by forest removal is not passed on to the atmosphere, which in fact means "no albedo change" in the atmosphere model since it takes in observed albedo data. The other biophysical variables are still being affected by deforestation. Thus, the albedo effect can be isolated by calculating the difference (ALL − noALB) between the regular global deforestation simulation (ALL) that includes the albedo change and the noALB experiment. In the noRGH experiment, roughness is set to be unaffected by forest clearing; therefore, the difference ALL − noRGH can be attributed to the roughness effect. The calculation of evapotranspiration involves many parameters. For example, both albedo and roughness can affect evapotranspiration (ET). Therefore, for the EVA experiment, a different strategy is adopted by fixing both albedo and roughness (as in CTL) while other variables are allowed to change. Thus, the difference between EVA and control, EVA − CTL, reflects processes other than albedo and roughness that can affect ET, representing the pure hydrological effect of deforestation that refers to the ability of vegetation to transfer water from the soil to the atmosphere (Davin and de Noblet-Ducoudré, 2010).

All deforestation simulations are initialized with the restart files after spin-up, whose vegetation map, relevant parameters, and model codes have been modified as described above. Each simulation is run for 100 years and the averaged results of the final 10 years are used for the analysis. Ground temperature is used to analyze temperature change because the model does not output the 2 m air temperature. Ground temperature has a strong signal of the locally induced temperature change, which is closely coupled to the surface energy balance. This enables us to focus on the local and regional impacts of vegetation change. Only model grid points with a forest fractional change larger than 0.1 are analyzed for robustness. The resulting changes in LAI, albedo, and roughness, induced by global deforestation, are provided in the Supplement (Figs. S3–S5).

3 Results

3.1 Latitudinal temperature change in response to deforestation

The latitude dependence of the temperature response is confirmed by the three regional deforestation experiments (see Fig. 1a–c for tropical, northern temperate, and boreal and Fig. 1d for global deforestation experiments). The deforestation impact in the simulation is a very strong signal relative to the small interannual variability, making almost all changes over land statistically significant. Therefore, significance levels are not shown on the map. In the tropical deforestation (20° S–20° N) experiment, a significant and widespread warming of 2.22 K (Table 2) is observed over deforested regions; this is greatest (∼4 K) in the Amazon and central African regions and about 1–2 K in southern Asia and the east coast of Australia. Although warming is the dominant effect, there are areas around the Sahel, northern Africa, in which we observe cooling up to −2 K. This suggests that temperature response can differ within a latitude band, as shown in earlier studies (McGuffie et al., 1995; Snyder et al., 2004). The regional difference is partly due to the regional circulation patterns being affected differently by deforestation (McGuffie et al., 1995). Temperature outside the deforestation boundary (e.g., southern Asia, northern Canada) is

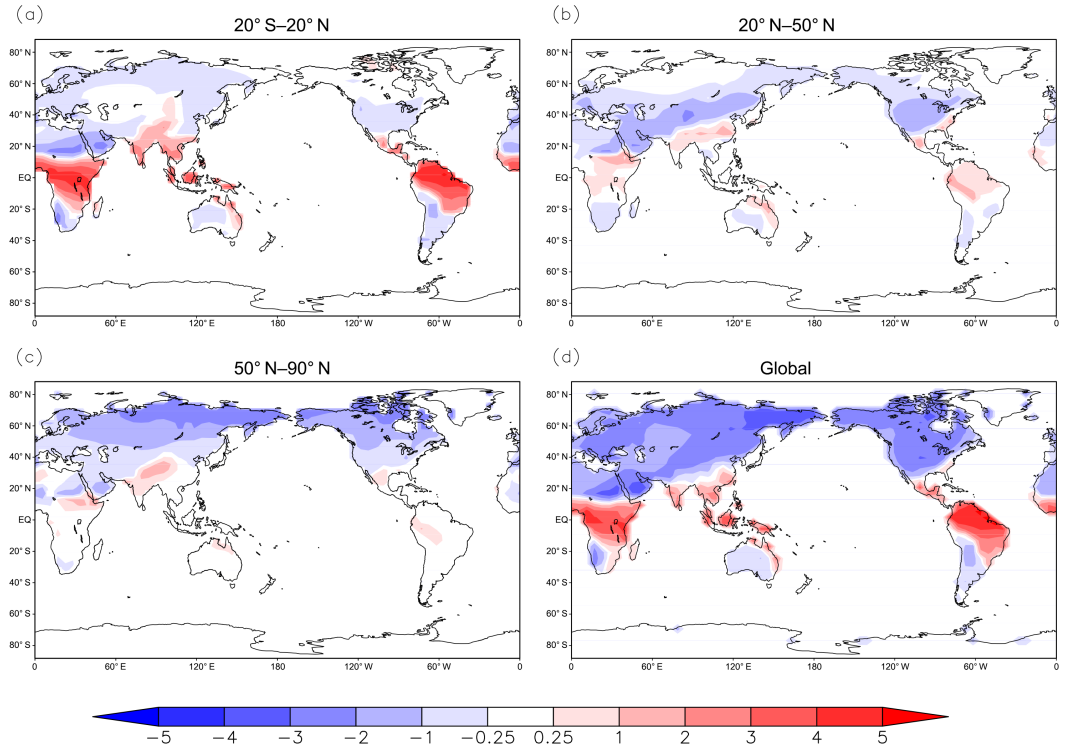

Figure 1. Ground temperature change for **(a)** tropical (20° S–20° N), **(b)** northern temperate (20–50° N), **(c)** boreal (50–90° N), and **(d)** global (90° S–90° N) deforestation (unit: K).

Table 2. Changes in key climate variables from regional and global deforestation experiments. "Δ" denotes change relative to the control experiment. The value for each climate variable is the area-weighted change over deforested areas for different latitude zones. The symbol "↑" denotes upward and "↓" denotes downward. Units are watts per square meter for energy flux, kelvin for temperature, millimeters per day for precipitation; albedo is unitless.

	Tropical (20° N–20° S)		Temperate (20–50° N)		Boreal (50–90° N)	
	Regional	Global	Regional	Global	Regional	Global
Temperature	2.22	2.06	−0.84	−1.56	−1.70	−2.42
Precipitation	−3.75	−3.89	−0.71	−0.89	−0.14	−0.21
ET	−82	−85	−17	−21	−5	−5
Sensible heat (ΔH)	15	13	−12	−13	−14	−14
Shortwave↓ (ΔSW↓)	50	53	18	21	13	14
Shortwave↑ (ΔSW↑)	88	95	41	48	37	38
Longwave↓ (ΔLW↓)	−14	−17	−11	−17	−6	−11
Net shortwave (ΔSW)	−38	−42	−23	−27	−24	−24
Albedo	0.26	0.28	0.17	0.18	0.22	0.22
Turbulent flux (ΔTub = ΔH+ΔET)	−67	−72	−29	−34	−19	−19
Available energy (ΔAva = ΔSW + LW↓)	−52	−59	−34	−44	−30	−35

also influenced by tropical deforestation, indicating that the vegetation disturbance signal can spread to distant regions through atmospheric processes. Replacing forest with bare ground leads to a surface albedo increase of 0.26 and a decrease of shortwave absorption at the surface by 38 W m^{-2}. Precipitation and evapotranspiration also decline drastically by 3.75 mm day^{-1} and 82 W m^{-2}, respectively, while sensible heat increases. Reducing cloud cover results in an increase in downward shortwave and a decrease in downward longwave radiation (Table 2).

In the northern temperate region (20–50° N), deforestation causes a temperature decrease of −0.84 K over most areas. North China and most parts of the United States show the largest cooling (∼ −1.5 K), while a weaker cooling (< −1 K) is observed in Europe. Nevertheless, temperature rise can be found in some areas, like southern China (1∼2 K) and the

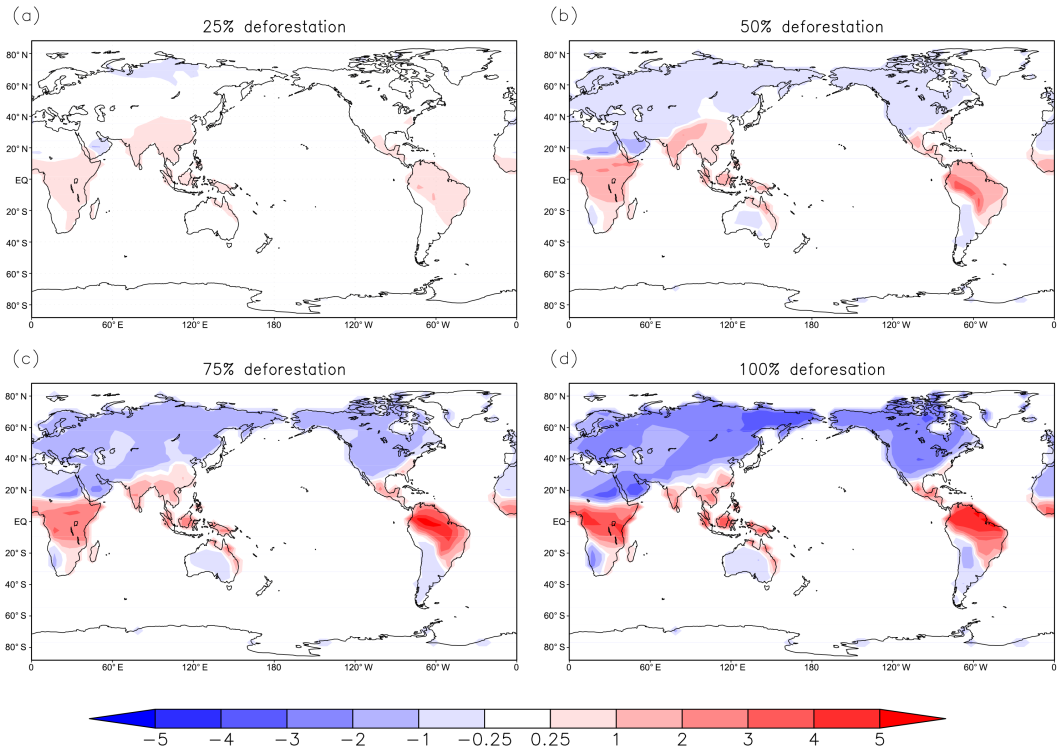

Figure 2. Temperature change for global deforestation experiments with different deforestation fractions at **(a)** 25 %, **(b)** 50 %, **(c)** 75 %, and **(d)** 100 %.

southeast US (∼1 K), similar to the tropics. The regional difference also reflects the different response of the surface energy balance to deforestation, and is related to the background climate as discussed in the next section. Other changes, including increased albedo and decreased shortwave absorption as well as a decrease in ET and precipitation, can be seen in temperate deforestation, but the magnitudes are much smaller than those in the tropics. Unlike the tropical region, sensible heat decreases in the temperate region and is consistent with the sign of temperature change.

Compared with the temperate region, deforestation in the boreal region results in a stronger cooling of −1.70 K but changes in the surface energy components are much smaller. It should be noted that albedo only increases by 0.22 because of no snow-masking effect in the land surface model, which could enhance the cooling signal by amplifying the albedo change. Nevertheless, a considerable cooling is seen in our results without the snow-masking effect, suggesting that changes other than snow contribute to the cooling effect of deforestation.

3.2 Sensitivity of temperature change to spatial extent and degree of vegetation change

The influence of spatial extent of deforestation can be clearly seen by comparing the temperature response in a given region under regional and global deforestation experiments. While similar in spatial pattern, temperature change in the global deforestation experiment (Fig. 1d) is much stronger than that in the regional deforestation, especially in mid- and high latitudes (Table 2). From the regional to global scale, deforestation-induced cooling increases from −0.84 to −1.56 K and from −1.70 to −2.42 K in the northern temperate and boreal regions, respectively. In contrast, warming in the tropics is less affected and even slightly decreases from 2.22 K in the regional deforestation case to 2.06 K in the global case. This is because global deforestation leads to a stronger reduction in both absorbed shortwave radiation and downward longwave radiation, both amplifying the cooling effects (Table 2) that reduce tropical warming and enhance high-latitude cooling. Such dampened tropical warming and enhanced extratropical cooling from regional to global deforestation experiments are supported by a recent study (Devaraju et al., 2015). Overall, an amplified temperature change in the global deforestation experiment is expected as it generates a stronger perturbation in the atmosphere, but the latitudinal temperature response is well preserved despite the increase in the spatial extent of deforestation from regional to global.

By looking at a set of experiments with varying deforestation fractions, we found temperature change is also sensitive to degree of vegetation change (see Fig. 2, Table 3). Deforestation fraction refers to the percentage of trees removed relative to the original coverage (25, 50, 75, and 100 %), which

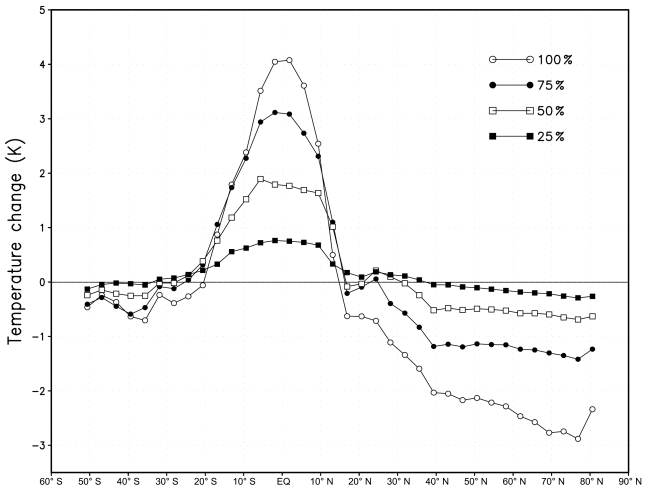

Figure 3. Latitudinal pattern of temperature change with different deforestation fractions.

is representative of the real areas that have been deforested. For 25 % deforestation fraction, temperature is virtually unaffected in most areas except for a weak warming in the tropics. As forest-loss fraction goes up to 50 %, a latitudinal temperature change emerges with discernible tropical warming and weak cooling in mid- and high latitudes (Fig. 3). Higher deforestation fractions of 75 and 100 % result in a greater temperature change and a more prominent latitudinal pattern. Generally, the magnitude of temperature change responds nonlinearly to increases in deforestation fraction, with much larger changes at high deforestation fractions (Fig. 3, Table 3). This nonlinearity can either arise from the response of biophysical land parameters to deforestation or from the climate response (i.e., temperature response) to biophysical changes. We found nonlinearities in both of these aspects (Fig. S6 in the Supplement).

3.3 Role of surface energy balance in latitudinal temperature change

Temperature change is driven by altered surface energy balance in response to forest removal. Among components of surface energy balance, changes in shortwave radiation absorption (ΔSW) and evapotranspiration (ΔET) can largely determine the sign and magnitude of temperature response to deforestation. Deforestation can increase surface albedo, leading to reduced absorbed shortwave radiation at the surface (ΔSW) which acts as a cooling mechanism, while decreased ET (ΔET) can produce a warming effect due to weakened latent cooling.

Figure 4c shows the latitudinal pattern of ΔSW and ΔET. Although the largest decreases are observed in the low latitudes and become smaller as latitude increases, the relative importance of these two varies across latitudes as also reported in Davin and de Noblet-Ducoudré (2010) and Li et al. (2015). In the tropics, ET declines (warming effect) more than the absorbed shortwave radiation (cooling effect). This ΔET-dominated energy imbalance is compensated for by an increase in temperature, outgoing longwave radiation, and sensible heat. Beyond the tropics, the opposite occurs, as ET declines less than absorbed shortwave radiation; therefore, temperature and sensible heat decrease in response to the ΔSW dominated energy imbalance. Specifically, the midlatitude are a transition region where ΔET and ΔSW in the south are relatively close to each other but quite different from each other in the north. In high latitudes, ΔET is negligible, whereas ΔSW maintains similar magnitude as in the midlatitudes, thus resulting in the most significant temperature decrease.

Although ΔSW and ΔET determine the basic latitudinal pattern of temperature change, changes in downward longwave radiation (ΔLW$\downarrow$) and sensible heat (ΔH) also have an influence. While ΔSW$\downarrow$ (changes in downward shortwave radiation) could be considered as a part of atmospheric feedback due to cloud cover change, we find that ΔSW is still dominated by ΔSW$\uparrow$ (changes in upward shortwave radiation) due to albedo change (Fig. S7 in the Supplement). ΔLW$\downarrow$ decreases across all latitudes due to less cloud cover, while sensible heat increases in the tropics and decreases in other latitudes. ΔLW$\downarrow$ is combined with ΔSW to give the available energy ($\Delta\text{Ava} = \Delta\text{SW} + \Delta\text{LW}\downarrow$) and ΔH is combined with ΔET to give the turbulence energy ($\Delta\text{Tub} = \Delta\text{ET} + \Delta\text{H}$), corresponding to the changes in received and dissipated energy, respectively. Available energy warms the land surface, while turbulence energy cools the surface (de Noblet-Ducoudré et al., 2012). The difference between these two is the outgoing longwave radiation, which is a function of ground temperature and is equivalent to ground temperature change. As shown in Fig. 4d, the latitudinal changes in the available and turbulence energy largely resemble that of ΔSW and ΔET but with some noticeable differences. Comparing with ΔSW, reduction in available energy (ΔAva) is larger across all latitudes, suggesting an amplifying feedback mechanism through ΔLW$\downarrow$ due to reduced cloud cover (more reduction in $\Delta\text{SW} + \Delta\text{LW}\downarrow$; Fig. 4a). However, ΔTub is smaller than ΔET in the tropics (less reduction for $\Delta\text{ET} + \Delta\text{H}$; Fig. 4b) but larger than ΔET in the mid- and high latitudes (more reduction for $\Delta\text{ET} + \Delta\text{H}$; Fig. 4b), showing that the warming signal can be either weakened or enhanced when ΔH is considered (see Table 2). Overall, the latitude pattern of ΔSW and ΔET in the Southern Hemisphere is influenced more by ΔLW$\downarrow$ and ΔH than in the Northern Hemisphere. In the Southern Hemisphere, the originally large energy difference between ΔSW and ΔET disappears when ΔLW$\downarrow$ and ΔH are accounted for, resulting in a dampened energy difference of ΔAve and ΔTub.

Analysis above shows that the basic latitudinal pattern of ΔSW and ΔET can explain most of the latitudinal temperature response regardless of other changes and feedbacks (e.g., changes in downward longwave radiation and sensible

Table 3. Changes in key climate variables from global deforestation with different deforestation fractions. "Δ" denotes change relative to the control experiment. The value for each climate variable is the area-weighted change over deforested areas for different latitude zones. The symbol "↑" denotes upward and "↓" denotes downward. Units are watts per square meter for energy flux, kelvin for temperature, millimeters per day for precipitation; albedo is unitless.

Region	Tropical (20° N–20° S)				Temperate (20–50° N)				Boreal (50–90° N)			
Deforestation fraction	25 %	50 %	75 %	100 %	25 %	50 %	75 %	100 %	25 %	50 %	75 %	100 %
Temperature	0.53	1.22	1.86	2.06	0.03	−0.23	−0.75	−1.56	−0.17	−0.55	−1.21	−2.42
Precipitation	−0.58	−1.54	−2.63	−3.89	−0.17	−0.49	−0.71	−0.89	−0.03	−0.07	−0.12	−0.21
ET	−15.3	−37.1	−59.2	−85.5	−4.6	−12.4	−17.4	−20.7	−0.6	−1.6	−2.6	−5.2
Sensible heat (ΔH)	12.0	23.2	27.8	13.3	2.4	0.9	−4.1	−13.3	−1.2	−3.6	−8.0	−14.1
Shortwave↓ (ΔSW↓)	3.8	13.1	27.1	52.6	1.7	7.7	14.1	21.3	1.4	3.9	7.7	13.8
Shortwave↑ (ΔSW↑)	3.0	16.1	40.5	94.9	2.6	14.8	29.7	48.3	3.5	9.8	20.2	37.8
Longwave↓ (ΔLW↓)	−0.7	−3.2	−6.7	−16.9	−1.2	−5.8	−10.6	−16.9	−0.8	−2.7	−5.6	−10.5
Albedo	0.01	0.05	0.12	0.28	0.01	0.06	0.11	0.18	0.02	0.06	0.12	0.22

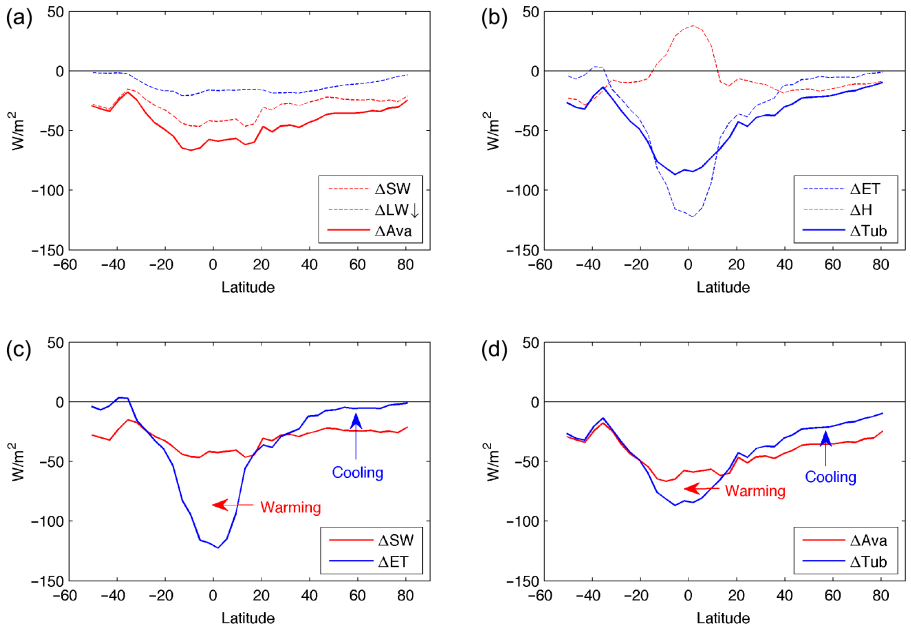

Figure 4. Latitudinal pattern of changes in surface energy balance. Panel **(a)**: changes in absorbed shortwave radiation (ΔSW), downward longwave radiation (ΔLW↓), and available energy (ΔAva = ΔSW + ΔLW↓). Panel **(b)**: changes in evapotranspiration (ΔET), sensible heat (ΔH), and turbulence energy (ΔTub = ΔET + ΔH). Panel **(c)**: ΔSW and ΔET. Panel **(d)**: ΔAva and ΔTub.

heat). Here we evaluate the extent to which the relative importance of ΔSW and ΔET can explain the spatially varying temperature change in terms of its sign and amplitude. The sign of temperature change can be approximated by a simple ratio of ΔET / ΔSW. The accuracy of this approximation depends on the strength of the basic pattern imposed by ΔSW and ΔET against other changes. A ratio larger than 1 suggests that ΔET warming exceeds ΔSW cooling and temperature is likely to increase, whereas a ratio smaller than 1 suggests that ΔSW cooling is stronger than ΔET warming and temperature tends to decrease. We used results from the regional deforestation numerical experiments to demonstrate this feature. Figure 5 shows the deforested grid points in the model with their ΔET and ΔSW plotted on the x and y axes, with colors representing the sign of temperature change. Deforested points with increased temperature (red) are often located in the upper-left space of the ΔET = ΔSW line where warming is anticipated (ΔET > ΔSW), while points with decreased temperature fall into the lower-right space where cooling is anticipated (ΔET < ΔSW). It turns out that ΔET and ΔSW alone can explain 93, 88, and 99 % of deforested points for the direction of temperature change in the tropical, temperate, and boreal regions, respectively. In addition, there is a tendency towards smaller ΔET / ΔSW ratios at higher latitudes and drier areas in the global deforestation experiment (Fig. S8 in the Supplement), suggesting a decreasing

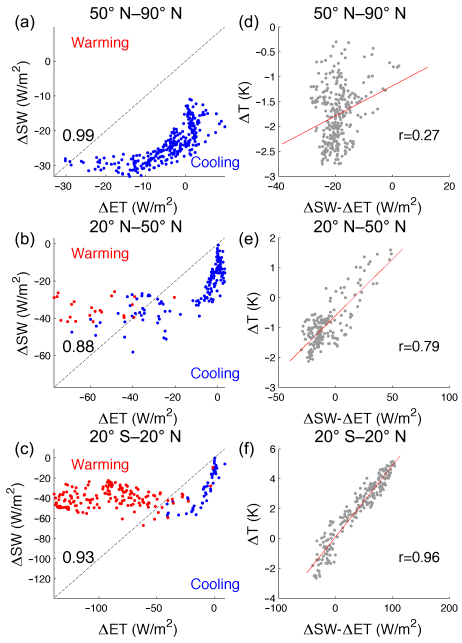

Figure 5. Changes in ET (ΔET), absorbed shortwave radiation (ΔSW), and their relationship with temperature change (ΔT) over deforestation areas. Panels **(a–c)**: deforested points with their ΔSW, ΔET, and the sign of ΔT. The upper left area represents ET warming exceeding albedo cooling; the lower-right area represents albedo cooling exceeding ET warming. Blue (red) are the actual grid points where temperature decreased (increased). Number denotes the percentage of deforested points whose sign of ΔT can be explained by the relative importance of ΔSW and ΔET. Panels **(d–f)**: spatial relationship between ΔSW − ΔET and the amplitude of ΔT. Red line is the regression line, and r is the correlation coefficient. Panels **(a, d)**: boreal deforestation; panels **(b, e)**: northern temperate deforestation; panels **(c, f)**: tropical deforestation.

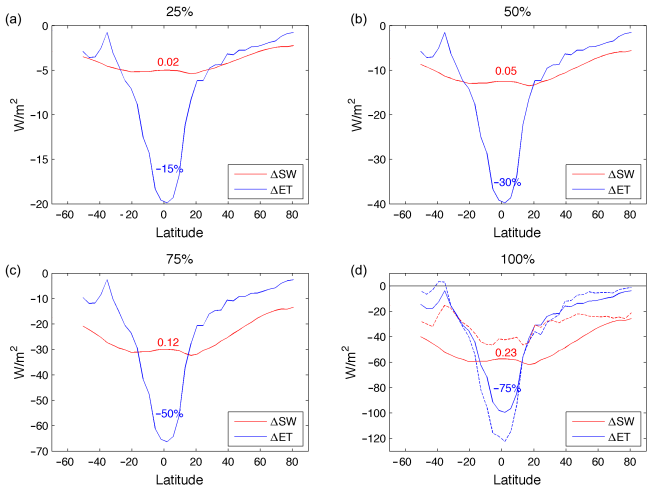

Figure 6. The latitudinal pattern of ΔSW and ΔET calculated by multiplying their background climate values with different rates for albedo (red number, from 0.02 in **(a)** to 0.23 in **d**) and ET changes (blue number, from −15 % in **(a)** to −75 % in **d**). In **(d)**, dashed lines are simulated changes from global deforestation for comparison with the calculated changes (solid line).

importance of ΔET over ΔSW. Few exceptions exist because longwave and sensible heat changes may also influence temperature change but are not considered here. Furthermore, the amplitude of temperature change is related to the difference of ΔSW and ΔET. As shown in Fig. 5d–f, ΔSW − ΔET is highly correlated with the amplitude of temperature change in the tropical ($r = 0.96$) and temperate regions ($r = 0.79$) but not in the boreal region ($r = 0.27$).

3.4 Influence of background climate on surface energy change and temperature change

The latitude-dependent pattern for ΔSW and ΔET could arise from the intrinsic latitudinal distribution in background climate, e.g., solar radiation and precipitation and ET decrease with latitude increase. Therefore, the same amount of albedo change would translate into a larger ΔSW in lower latitudes due to the geographic distribution of solar radiation. Likewise, given the same ET reduction rate, a larger ΔET is expected in the tropics than in high latitudes.

The influence of background climate can be illustrated by a simple calculation. Assume that deforestation causes an albedo increase of 0.02, 0.05, 0.12, and 0.23 uniformly across all latitudes and an ET decrease of 15, 30, 50, and 75 % compared to its baseline climatology, respectively. Multiplying these change rates by the baseline shortwave radiation and ET, we obtain the corresponding ΔSW and ΔET without considering any climate feedback. For demonstration purposes, the change rates chosen here for albedo and ET roughly correspond to the global averaged changes in the four deforestation fraction experiments (deforestation fraction ranges from 25 to 100 %; see group II experiment). Interestingly, the calculated ΔSW and ΔET (Fig. 6) agree well with the simulation (Fig. 4c). The main features, including ΔET > ΔSW in the tropics and ΔET < ΔSW in the extratropics, are captured. We also used the satellite-derived ET and shortwave radiation data from Li et al. (2015) to perform the calculation (see Fig. S9 in the Supplement). The results generally support the findings from Fig. 6, except for the two combinations with small changes in albedo and ET. For these two cases, the anticipated pattern is not captured mainly because of the chosen low albedo change in high latitude, which leads to an underestimation of ΔSW. It should be emphasized that the albedo and ET change rates in reality have more complicated patterns than what we assume in the calculation. Nevertheless, our simple calculation still reveals the role of the baseline climate in shaping the latitude-dependent temperature change to deforestation.

Further evidence comes from the spatial relationship between background climate and temperature response to deforestation. We found baseline precipitation is highly corre-

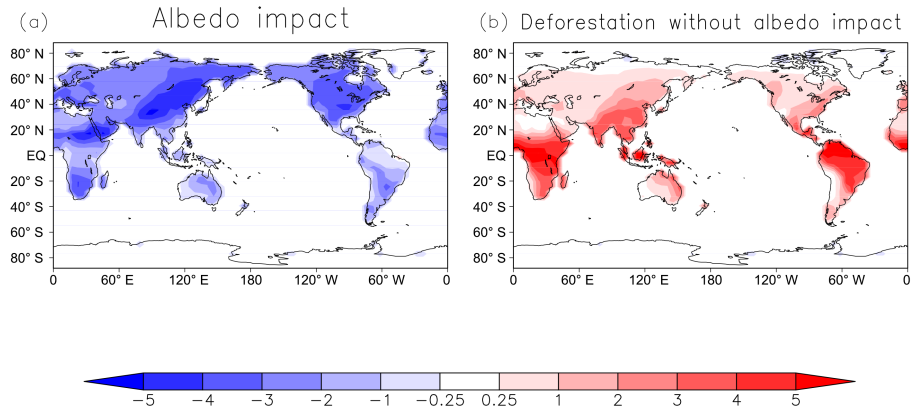

Figure 7. Panel **(a)**: impact of albedo (only) on temperature change; panel **(b)**: temperature change without albedo impact (K).

lated with ΔET ($r = -0.98$) and with ΔT ($r = 0.87$), suggesting that precipitation can influence temperature change by controlling ET change. This is also supported by the ratio of ΔET / ΔSW in Fig. S8 in the Supplement where larger ΔET over ΔSW is found in wetter areas and by observations from air temperature (Zhang et al., 2014) and physical mechanisms pertaining to soil moisture (Swann et al., 2012). Therefore, spatial variation of temperature change is partly due to background climate. For instance, temperature decreases in the tropical deforested areas like the Sahel, west Amazon, and southwestern Africa because dry climate limits ΔET; thus, temperature change is dominated by the cooling effect from ΔSW. In contrast, in wet temperate deforested areas like southern China, India, and parts of North America, temperature increases because of the dominant warming effect from ΔET.

3.5 Contribution of individual biophysical processes to the latitudinal temperature change

The aforementioned changes in temperature and surface energy balance are triggered by the altered biophysical variables such as albedo, roughness, and ET efficiency as a result of deforestation. The effect of each individual biophysical factor and its contribution to temperature change are evaluated in this section.

1. Albedo

   The impact of albedo change can be isolated by the difference of ALL − noALB (see the "Method" section), as shown in Fig. 7a. As expected, albedo change causes significant temperature decrease over all affected regions. Surprisingly, the strongest cooling appears in the northern temperate region instead of the tropics where the largest albedo increase occurs (Table 4). This indicates that the strength of perturbation is not the only factor for determining spatially varying temperature change. The magnitude of cooling in the boreal region is similar to the temperate region because of no amplified albedo change due to snow. If deforestation did not change albedo, there would be a substantial warming over all affected regions (noALB − CTL; Fig. 7b), accompanied with decreased ET and very little change in absorbed shortwave radiation (SW). This is expected because the warming effect of ΔET dominates temperature change when the albedo effect is absent.

2. Roughness

   Roughness can affect turbulence (ET as well as sensible heat) flux between land surface and atmosphere. Higher roughness facilitates absorbed shortwave energy to be dissipated as turbulence, while smaller roughness suppresses this process and could have a warming effect. The effect of roughness on climate can be isolated by the difference All − noRGH. Roughness change as well as its impact are more pronounced in the tropical region (Table 4). As is seen in Fig. 8a, reduced roughness warms most areas except for the upper northern latitudes, with warming decreasing from the tropics to high latitudes; see also Davin and de Noblet-Ducoudré (2010). Without roughness change, deforestation would cause less warming (Fig. 8b) and less reduction in turbulence energy (not shown) than regular deforestation. Moreover, Fig. 8b also shows the combined effects of albedo and evapotranspiration efficiency since the roughness effect is excluded. Thus, the existence of a tropical warming in some regions implies that the reduction in evapotranspiration efficiency remains dominant and outweighs the albedo impact in this situation.

3. Evapotranspiration efficiency

   Evapotranspiration efficiency refers to the ability of partitioning available energy into evapotranspiration more than into sensible heat. The conversion of forest to bare land favors more turbulence energy to be transferred in the form of sensible heat rather than ET, resulting in higher Bowen ratio. The impact of altered ET efficiency

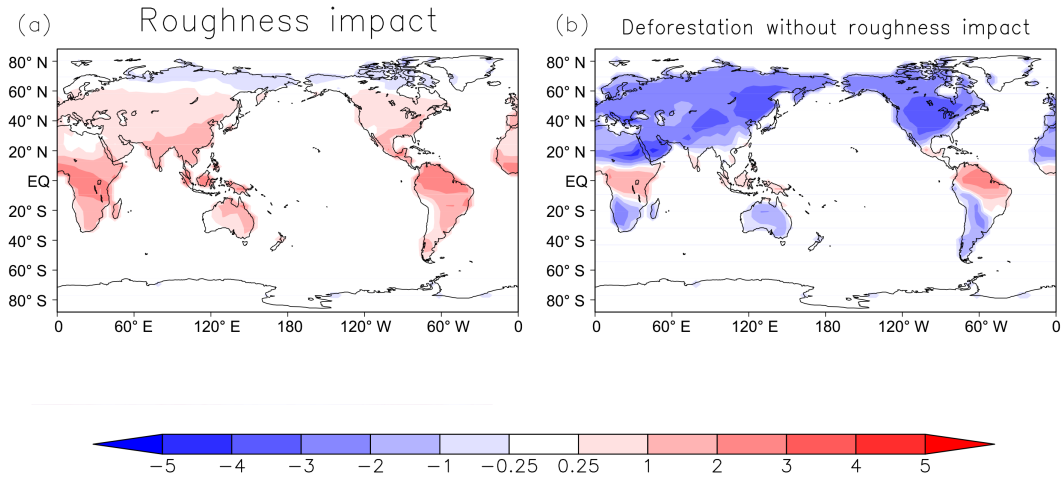

Figure 8. Panel **(a)**: impact of roughness (only) on temperature; panel **(b)**: temperature change without roughness (K).

Table 4. Summary of the influence of individual biophysical factors on temperature change (K). Numbers in parentheses are changes in albedo and roughness. Albedo is unitless, and the unit for roughness is meters.

	Global (ALL − CTL)	Albedo (ALL − noALB)	Roughness (ALL − noRGH)	Evapotranspiration efficiency (EVA − CTL)
50–90° N	−2.42	−2.93 (0.22)	0.05 (0.86)	0
20–50° N	−1.56	−3.1 (0.18)	0.86 (0.66)	0.27
20° S–20° N	2.06	−1.92 (0.28)	1.92 (1.33)	1.22

ALL: global deforestation; noALB: global deforestation without albedo change; noRGH: global deforestation without roughness change; EVA: global deforestation without both albedo and roughness change.

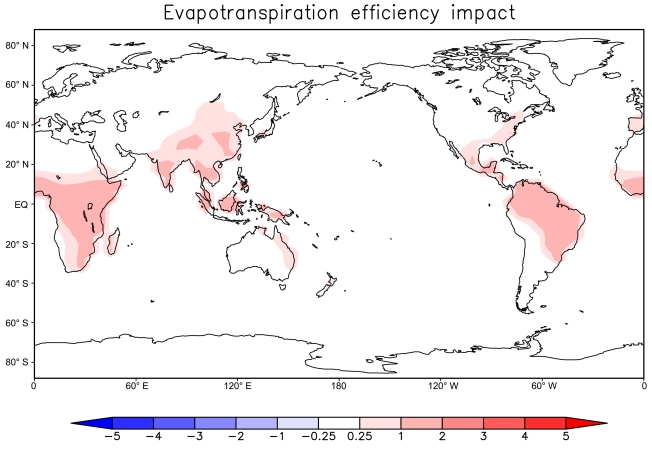

Figure 9. Evapotranspiration efficiency impact on temperature change (K).

can be separated by EVA − CTL, showing a noticeable warming in the tropical regions and some parts of the temperate region and negligible impact in high latitude (Fig. 9). It seems that changed ET efficiency has a significant impact only over regions with wet climate, which may be due to the close coupling between precipitation and ET change.

By summing up the contributions from individual biophysical factors linearly (ALL − noALB + ALL − noRGH + EVA − CTL), we reconstruct temperature change, which closely agrees with the actual signal (ALL − CTL) in terms of both latitudinal (Fig. 10) and geographical patterns (Fig. 11). Latitudinal features are inherited in the contribution of each individual component (Table 4). The albedo effect generally increases with latitude, whereas roughness and evapotranspiration efficiency effects decrease with latitude. Therefore, the largest temperature increase in the tropical region (2.06 K) originates from the warming effect of changed roughness (1.92 K) and evapotranspiration efficiency (1.22 K) and is counteracted by a comparatively small albedo cooling (−1.92 K). In the extratropics, the temperature response is dominated by albedo cooling, with similar strengths in the northern temperate (−3.01 K) and boreal (−2.93 K) regions. But such cooling is partially canceled by the weaker warming effect of roughness (0.86 K) and evapotranspiration efficiency (0.27 K) in the temperate region and no compensation at all in the boreal region. The latitudinal pattern caused by each biophysical factor is less likely to be due to the latitudinal signal from biophysical change per se

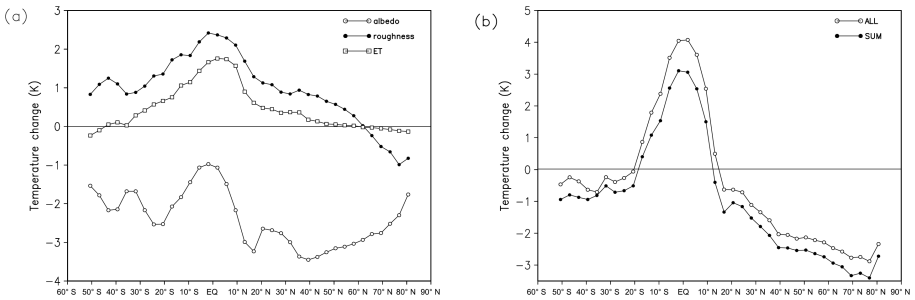

Figure 10. Panel **(a)**: latitudinal patterns of the contribution of individual biophysical factors to temperature change and **(b)** reconstructed temperature change from individual biophysical effects (SUM = ALL − noALB + ALL − noRGH + EVA − CTL).

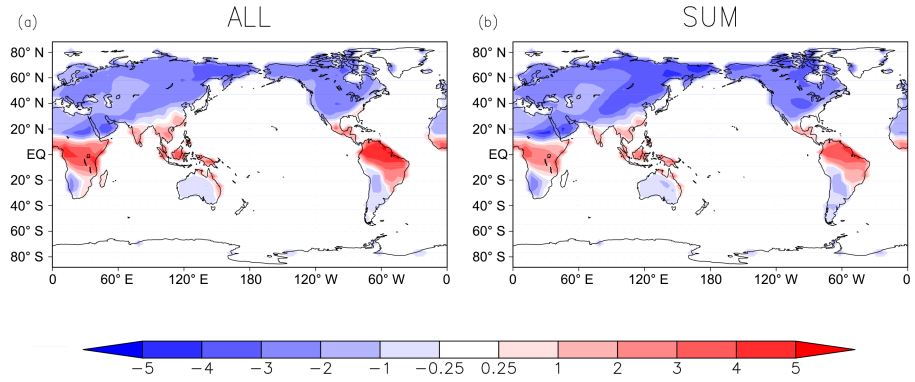

Figure 11. Spatial patterns of **(a)** actual temperature change and **(b)** reconstructed temperature change (SUM = ALL − noALB + ALL − noRGH + EVA − CTL). Unit is Kelvin for temperature.

because biophysical change does not match the latitude pattern of temperature response. For example, the largest temperature change does not occur where the largest biophysical change (e.g., albedo and roughness) occurs. This shows the complex interactions in the translation from the initial perturbation to subsequent climate response, which varies by latitude. Biophysical impacts are strongly regulated by the baseline climate where vegetation change occurs, as also demonstrated in Pitman et al. (2011).

4 Discussion

Our results show patterns of temperature change as a result of deforestation that are in line with the conclusions of previous modeling studies, e.g., strong tropical warming (Nobre et al., 1991; Snyder et al., 2004), moderate temperate cooling, and strong boreal cooling (Bonan et al., 1992, 1995; Betts, 2000), but few of them consider the spatial scale of deforestation. We found that temperature change varies nonlinearly with both the spatial scale and the fraction of forest removed, with increasingly larger temperature change as disturbance grows, but the overall latitudinal pattern is not altered. This scale-dependent relationship between temperature change and deforestation reflects a perturbation–response relationship derived from the existing mechanisms of the model in which nonlinearity is found. However, it does not exactly emulate the influence of physical processes operating on various scales in the real world because many scale-related processes cannot be fully resolved in a model with a fixed complexity. For example, many mesoscale processes cannot be included in a global model. This makes it difficult to compare our results to observational study results that span different spatial scales.

We found that changes in shortwave radiation absorption (ΔSW) and evapotranspiration (ΔET) can largely determine the sign and amplitude of temperature change, as well as its latitudinal and spatial patterns in response to deforestation. In a global deforestation scenario, more than 90 % of the sign of temperature change over deforested areas can be explained by ΔSW and ΔET. Although ΔET and ΔSW can be influenced by other factors and feedbacks, they still provide useful diagnostic information for temperature change and serve as a first-order approximation. Using this information, albedo and ET changes (two variables readily available from satellite data) can be potentially applied to evaluate the possible impact of ongoing land cover change on local and regional temperature (Loarie et al., 2011; Peng et al., 2014; Li et al., 2015).

To a large extent, the latitude-dependent temperature response to deforestation and its spatial variability can be at-

tributed to background climate conditions, such as solar radiation, precipitation, and snow, which in turn affect the biophysical impact of vegetation change. Further evidence comes from the contribution of each biophysical factor, i.e., albedo, roughness, and ET efficiency, to the temperature response. Although these factors drive temperature change in different directions, their contributions also have clear latitudinal patterns (Davin and de Noblet-Ducoudré, 2010). This indicates that the climate condition manifests its influence either explicitly in the temperature response through controlling changes in surface energy balance or implicitly in the magnitude of biophysical alteration triggered by deforestation. After careful analysis of our model, our results show that the latitudinal pattern of temperature change is due to the explicit impact of the climate condition.

We acknowledge certain limitations and important issues that are not fully addressed in this study. Previous studies showed an important role of oceanic feedback, which could cause additional cooling through albedo change (e.g., sea-ice albedo feedback) and could override temperature change over land in midlatitudes (Claussen et al., 2001; Davin and de Noblet-Ducoudré, 2010), but our ocean model is not interactive so such dynamics could not be studied here. In the simulation, we used the SST climatology of 1960–1990 with a seasonal cycle only that can minimize interannual variability and therefore amplify the strength of deforestation signal to climate variability in terms of statistical significance. If a different period of the SST climatology had been used, the simulated climate may have been slightly different, including differences in vegetation distribution and deforestation impacts. Nevertheless, our results are unlikely to be substantially changed by the choice of SST climatology because a background climate change as large as that coming from $1 \times CO_2$ (280 ppm) increased to $2 \times CO_2$ (560 ppm) can only modify the climate impact over certain transitional regions (Pitman et al., 2011).

Furthermore, in this study we use ground temperature as the variable for accessing the deforestation impact. In other studies, and perhaps more commonly, this component could be analyzed using air temperature, although research based on ground temperature (McGuffie et al., 1995; Kendra Gotangco Castillo and Gurney, 2012) or surface temperature (Davin and de Noblet-Ducoudré, 2010) is also seen in the literature. Although these two have been shown to often agree with one another on larger scales (Jin et al., 1997), it is worth investigating whether they have different responses to vegetation change (Baldocchi and Ma, 2013; Zhao and Jackson, 2014; Li et al., 2015). Moreover, the response of maximum and minimum temperatures also differs from the daily average temperature (Zhang et al., 2014; Li et al., 2015), a problem that has received less attention in modeling studies.

Finally, results from a single model are subject to uncertainty and some features might be model-dependent. For instance, some biases in the simulated climate of the model may lead to shifts in vegetation distribution and thus could influence the deforestation impact. To combat this, model intercomparison projects like Land-Use and Climate, Identification of Robust Impacts (LUCID) experiments (Pitman et al., 2009) can help to distinguish robust findings from model uncertainty. The participant models in LUCID show consistency in how land cover change affects available energy but diverge greatly on energy partition between latent and sensible heat flux changes (de Noblet-Ducoudré et al., 2012), indicating that large uncertainty lies in the response of non-radiative process to land cover change, especially for ET (Boisier et al., 2012). Therefore, considerable effort is required to improve model performance in the simulation of land processes, and new intercomparison projects such as LUMIP (Land Use Model Intercomparison Project, https://cmip.ucar.edu/lumip) are highly valuable. In addition, observational studies are indispensable as they can offer new insights and serve as a reference benchmark for model results, especially those using new techniques and data sets such as satellite data.

The Supplement related to this article is available online at doi:10.5194/esd-7-167-2016-supplement.

Author contributions. Y. Li designed and carried out the experiments; Y. Li and N. De Noblet-Ducoudré analyzed the data; all authors contributed to the discussion and writing of the paper.

Acknowledgements. This work is supported by the National Basic Research Program of China (Grant No. 2015CB4527022), the National Natural Science Foundation of China (Grant No. 41130534 and 41371096), and the Maryland Council on the Environment. Y. Li also received support from the China Scholar Council (Fellowship No. 201306010169). S. Motesharrei received support from the National Socio-Environmental Synthesis Center (SESYNC)–NSF award DBI-1052875. We thank Andy Pitman for his constructive and insightful comments on this paper. Y. Li thanks Fang Zhao for his help with the model simulations. We thank Laura Bracaglia for careful reading of the manuscript and helpful edits in the writing. We are grateful to the two anonymous reviewers for their helpful comments and suggestions.

Edited by: A. Rammig

References

Allen, C. D., Macalady, A. K., Chenchouni, H., Bachelet, D., McDowell, N., Gonzalez, P., Fensham, R., Zhang, Z., Castro, J., Demidova, N., Lim, J.-H., Allard, G., Running, S. W., Semerci, A., and Cobb, N.: A global overview of drought and heat-induced tree mortality reveals emerging climate change risks for forests, Forest Ecol. Manage., 259, 660–684, 2010.

Avissar, R., Silva Dias, P. L., Sivla Dias, M. A. F., and Nobre, C.: The Large-Scale Biosphere-Atmosphere Experiment in Amazonia (LBA): Insights and future research needs, J. Geophys. Res., 107, 1–6, 2002.

Baidya Roy, S. and Avissar, R.: Impact of land use/land cover change on regional hydrometeorology in Amazonia, J. Geophys. Res., 107, 8037, doi:10.1029/2000JD000266, 2002.

Bala, G., Caldeira, K., Wickett, M., Phillips, T. J., Lobell, D. B., Delire, C., and Mirin, A.: Combined climate and carbon-cycle effects of large-scale deforestation, P. Natl. Acad. Sci. USA, 104, 6550–6555, 2007.

Baldocchi, D. and Ma, S.: How will land use affect air temperature in the surface boundary layer? Lessons learned from a comparative study on the energy balance of an oak savanna and annual grassland, Tellus B, 1, 1–19, 2013.

Betts, R. A.: Offset of the potential carbon sink from boreal forestation by decreases in surface albedo, Nature, 408, 187–190, 2000.

Betts, R. A., Falloon, P. D., Goldewijk, K. K., and Ramankutty, N.: Biogeophysical effects of land use on climate: Model simulations of radiative forcing and large-scale temperature change, Agr. Forest Meteorol., 142, 216–233, 2007.

Boisier, J. P., de Noblet-Ducoudré, N., Pitman, A. J., Cruz, F. T., Delire, C., van den Hurk, B. J. J. M., van der Molen, M. K., Müller, C., and Voldoire, A.: Attributing the impacts of land-cover changes in temperate regions on surface temperature and heat fluxes to specific causes: Results from the first LUCID set of simulations, J. Geophys. Res.-Atmos., 117, D12116, doi:10.1029/2011JD017106, 2012.

Bonan, G. B.: Forests and climate change: Forcings, feedbacks, and the climate benefits of forests, Science, 320, 1444–1449, 2008.

Bonan, G. B., Pollard, D., and Thompson, S. L.: Effects of Boreal Forest Vegetation on Global Climate, Nature, 359, 716–718, 1992.

Bonan, G. B., Chapin, F. S., and Thompson, S. L.: Boreal Forest and Tundra Ecosystems as Components of the Climate System, Clim. Change, 29, 145–167, 1995.

Bounoua, L., DeFries, R., Collatz, G. J., Sellers, P., and Khan, H.: Effects of land cover conversion on surface climate, Clim. Change, 52, 29–64, 2002.

Claussen, M., Brovkin, V., and Ganopolski, A.: Biogeophysical versus biogeochemical feedbacks of large-scale land cover change. Geophys. Res. Lett., 28, 1011–1014, 2001.

Darnell, W. L., Staylor, W. F., Gupta, S. K., Ritchey, N. A., and Wilber, A. C.: Seasonal variation of surface radiation budget derived from International Satellite Cloud Climatology Project C1 data, J. Geophys. Res.-Atmos., 97, 15741–15760, 1992.

Davin, E. L. and de Noblet-Ducoudré, N.: Climatic Impact of Global-Scale Deforestation: Radiative versus Nonradiative Processes, J. Climate, 23, 97–112, 2010.

de Noblet-Ducoudré, N., Boisier, J.-P., Pitman, A., Bonan, G. B., Brovkin, V., Cruz, F., Delire, C., Gayler, V., van den Hurk, B. J. J. M., Lawrence, P. J., van der Molen, M. K., Müller, C., Reick, C. H., Strengers, B. J., and Voldoire, A.: Determining Robust Impacts of Land-Use-Induced Land Cover Changes on Surface Climate over North America and Eurasia: Results from the First Set of LUCID Experiments, J. Climate, 25, 3261–3281, 2012.

Devaraju, N., Bala, G., and Modak, A.: Effects of large-scale deforestation on precipitation in the monsoon regions: Remote versus local effects, P. Natl. Acad. Sci., 112, 3257–3236, 2015.

Friedlingstein, P., Cox, P., Betts, R., Bopp, L., von Bloh, W., Brovkin, V., Cadule, P., Doney, S., Eby, M., Fung, I., Bala, G., John, J., Jones, C., Joos, F., Kato, T., Kawamiya, M., Knorr, W., Lindsay, K., Matthews, H. D., Raddatz, T., Rayner, P., Reick, C., Roeckner, E., Schnitzler, K.-G., Schnur, R., Strassmann, K., Weaver, A. J., Yoshikawa, C., and Zeng, N.: Climate–Carbon Cycle Feedback Analysis: Results from the C4MIP Model Intercomparison, J. Climate, 19, 3337–3353, 2006.

Gibbard, S., Caldeira, K., Bala, G., Phillips, T. J., and Wickett, M.: Climate effects of global land cover change. Geophys. Res. Lett., 32, L23705, doi:10.1029/2009GL039076, 2005.

Hales, K., Neelin, J. D., and Zeng, N.: Sensitivity of Tropical Land Climate to Leaf Area Index: Role of Surface Conductance versus Albedo, J. Climate, 17, 1459–1473, 2004.

Hansen, M., Potapov, P., and Moore, R.: High-resolution global maps of 21st-century forest cover change, Science, 850, 850–853, 2013.

Jin, M., Dickinson, R., and Vogelmann, A.: A comparison of CCM2-BATS skin temperature and surface-air temperature with satellite and surface observations, J. Climate, 10, 1505–1524, 1997.

Juang, J. Y., Katul, G., Siqueira, M., Stoy, P., and Novick, K.: Separating the effects of albedo from eco-physiological changes on surface temperature along a successional chronosequence in the southeastern United States, Geophys. Res. Lett., 34, L21408, doi:10.1029/2007GL031296, 2007.

Kendra Gotangco Castillo, C. and Gurney, K. R.: Exploring surface biophysical-climate sensitivity to tropical deforestation rates using a GCM: A feasibility study, Earth Int., 16, 1–23, 2012.

Lean, J. and Rowntree P.: Understanding the sensitivity of a GCM simulation of Amazonian deforestation to the specification of vegetation and soil characteristics, J. Climate, 10, 1216–1235, 1997.

Lee, X., Goulden, M. L., Hollinger, D. Y., Barr, A., Black, T. A., Bohrer, G., Bracho, R., Drake, B., Goldstein, A., Gu, L. H., Katul, G., Kolb, T., Law, B. E., Margolis, H., Meyers, T., Monson, R., Munger, W., Oren, R., Kyaw, T. P. U., Richardson, A. D., Schmid, H. P., Staebler, R., Wofsy, S., and Zhao, L.: Observed increase in local cooling effect of deforestation at higher latitudes, Nature, 479, 384–387, 2011.

Li, Y., Zhao, M., Motesharrei, S., Mu, Q., Kalnay, E., and Li, S.: Local cooling and warming effects of forest based on satellite data, Nature Comm., 6, 6603, doi:10.1038/ncomms7603, 2015.

Loarie, S. R., Lobell, D. B., Asner, G. P., Mu, Q., and Field, C. B.: Direct impacts on local climate of sugar-cane expansion in Brazil, Nature Clim. Change, 1, 105–109, 2011.

Longobardi, P., Montenegro, A., Beltrami, H., and Eby, M.: Spatial scale dependency of the modelled climatic response to deforestation, Biogeosciences Discuss., 9, 14639–14687, doi:10.5194/bgd-9-14639-2012, 2012.

Maynard, K. and Royer J.-F.: Sensitivity of a general circulation model to land surface parameters in African tropical deforestation experiments, Clim. Dynam., 22, 555–572, 2004.

McGuffie, K., Henderson-Sellers, A., Zhang, H., Durbidge, T. B., and Pitman, A. J.: Global climate sensitivity to tropical deforestation, Global Planet. Change, 10, 97–128, 1995.

Neelin, J. D. and Zeng, N.: A Quasi-Equilibrium Tropical Circulation Model—Formulation, J. Atmos. Sci., 57, 1741–1766, 2000.

Nobre, C., Sellers, P., and Shukla, J.: Amazonian Deforestation and Regional Climate Change, J. Climate, 4, 957–998, 1991.

Peng, S.-S., Piao, S., Zeng, Z., Ciais, P., Zhou, L., Li, L. Z. X., Myneni, R. B., Yin, Y., and Zeng, H.: Afforestation in China cools local land surface temperature, P. Natl. Acad. Sci. USA, 111, 2915–2919, 2014.

Pitman, A. J., de Noblet-Ducoudré, N., Cruz, F. T., Davin, E. L., Bonan, G. B., Brovkin, V., Claussen, M., Delire, C., Ganzeveld, L., Gayler, V., van den Hurk, B. J. J. M., Lawrence, P. J., van der Molen, M. K., Müller, C., Reick, C. H., Seneviratne, S. I., Strengers, B. J., and Voldoire, A.: Uncertainties in climate responses to past land cover change: First results from the LUCID intercomparison study, Geophys. Res. Lett., 36, L14814, doi:10.1029/2009GL039076, 2009.

Pitman, A. J., Avila, F. B., Abramowitz, G., Wang, Y. P., Phipps, S. J., and de Noblet-Ducoudré, N.: Importance of background climate in determining impact of land-cover change on regional climate, Nature Clim. Change, 1, 472–475, 2011.

Pitman, A. J., Arneth, A., and Ganzeveld, L.: Regionalizing global climate models, Int. J. Climatol., 32, 321–337, 2012.

Rayner, N. A., Brohan, P., Parker, D. E., Folland, C. K., Kennedy, J. J., Vanicek, M., Ansell, T. J., and Tett, S. F. B.: Improved analyses of changes and uncertainties in sea surface temperature measured in Situ since the mid-nineteenth century: The HadSST2 dataset, J. Climate, 19, 446–469, 2006.

Runyan, C. () Physical and biological feedbacks of deforestation, Rev. Geophys., 50, 1–32, 2012.

Sampaio, G., Nobre, C., Costa, M. H., Satyamurty, P., Soares-Filho, B. S., and Cardoso, M.: Regional climate change over eastern Amazonia caused by pasture and soybean cropland expansion, Geophys. Res. Lett., 34, L17709, doi:10.1029/2007GL030612, 2007.

Snyder, P. K.: The Influence of Tropical Deforestation on the Northern Hemisphere Climate by Atmospheric Teleconnections, Earth Int., 14, 1–34, 2010.

Snyder, P. K., Delire, C., and Foley, J. A.: Evaluating the influence of different vegetation biomes on the global climate, Clim. Dynam., 23, 279–302, 2004.

Souza, D. C. and Oyama, M. D.: Climatic consequences of gradual desertification in the semi-arid area of Northeast Brazil, Theor. Appl. Climatol., 103, 345–357, 2010.

Swann, A. L. S., Fung, I. Y., and Chiang, J. C. H.: Mid-latitude afforestation shifts general circulation and tropical precipitation, P. Natl. Acad. Sci. USA, 109, 712–716, 2012.

Wickham, J. D., Wade, T. G., and Riitters, K. H.: Empirical analysis of the influence of forest extent on annual and seasonal surface temperatures for the continental United States, Global Ecol. Biogeogr., 22, 620–629, 2013.

Zeng, N.: Glacial-interglacial atmospheric CO_2 change – The glacial burial hypothesis, Adv. Atmos. Sci., 20, 677–693, 2003.

Zeng, N.: How strong is carbon cycle-climate feedback under global warming?, Geophys. Res. Lett., 31, L20203, doi:10.1029/2004GL020904, 2004.

Zeng, N. and Neelin, J. D.: The Role of Vegetation Climate Interaction and Interannual Variability in Shaping the African Savanna, J. Climate, 13, 2665–2670, 2000.

Zeng, N. and Yoon, J.: Expansion of the world's deserts due to vegetation-albedo feedback under global warming, Geophys. Res. Lett., 36, L17401, doi:10.1029/2009GL039699, 2009.

Zeng, N., Neelin, J. D., Lau, K. M., and Tucker, C. J.: Enhancement of Interdecadal Climate Variability in the Sahel by Vegetation Interaction, Science, 286, 1537–1540, 1999.

Zeng, N., Neelin, J. D., and Chou, C.: A Quasi-Equilibrium Tropical Circulation Model—Implementation and Simulation, J. Atmos. Sci., 57, 1767–1796, 2000.

Zeng, N., Mariotti, A., and Wetzel, P.: Terrestrial mechanisms of interannual CO_2 variability, Global Biogeochem. Cy., 19, 1–15, 2005.

Zhang, M., Lee, X., Yu, G., Han, S., Wang, H., Yan, J., Zhang, Y., Li, Y., Ohta, T., Hirano, T., Kim, J., Yoshifuji, N., and Wang, W.: Response of surface air temperature to small-scale land clearing across latitudes, Environ. Res. Lett., 9, 034002, doi:10.1088/1748-9326/9/3/034002, 2014.

Zhao, K. and Jackson, R.: Biophysical forcings of land-use changes from potential forestry activities in North America, Ecol. Monogr., 84, 329–353, 2014.